Mechanical properties of functionalized carbon nanotubes

2008 Nanotechnology 19 395702

(http://iopscience.iop.org/0957-4484/19/39/395702)

Nanotechnology **19** (2008) 395702 (6pp) doi:10.1088/0957-4484/19/39/395702

Mechanical properties of functionalized carbon nanotubes

Z Q Zhang[1], B Liu[1,5], Y L Chen[1], H Jiang[2], K C Hwang[1] and Y Huang[3,4,5]

[1] FML, Department of Engineering Mechanics, Tsinghua University, Beijing 100084, People's Republic of China
[2] Department of Mechanical and Aerospace Engineering, Arizona State University, Tempe, AZ 85287, USA
[3] Department of Civil and Environmental Engineering, Northwestern University, Evanston, IL 60208, USA
[4] Department of Mechanical Engineering, Northwestern University, Evanston, IL 60208, USA

E-mail: liubin@tsinghua.edu.cn and y-huang@northwestern.edu

Received 4 May 2008, in final form 20 July 2008
Published 11 August 2008
Online at stacks.iop.org/Nano/19/395702

Abstract
Carbon nanotubes (CNTs) used to reinforce polymer matrix composites are functionalized to form covalent bonds with the polymer in order to enhance the CNT/polymer interfaces. These bonds destroy the perfect atomic structures of a CNT and degrade its mechanical properties. We use atomistic simulations to study the effect of hydrogenization on the mechanical properties of single-wall carbon nanotubes. The elastic modulus of CNTs gradually decreases with the increasing functionalization (percentage of C–H bonds). However, both the strength and ductility drop sharply at a small percentage of functionalization, reflecting their sensitivity to C–H bonds. The cluster C–H bonds forming two rings leads to a significant reduction in the strength and ductility. The effect of carbonization has essentially the same effect as hydrogenization.

1. Introduction

Carbon nanotubes (CNTs) possess superior physical and mechanical properties such as low mass density (1.3–1.4 g cm^{-3}) [1], large aspect ratio (>a few hundreds) [2], high Young's modulus (∼1 TPa) [3–16], strength (∼30 GPa) [5–8] and large fracture strain (>10%) [5, 6, 17, 18]. They are an ideal candidate for reinforcements in nanocomposites [1, 2, 19–24].

Prior experimental and numerical studies of CNT-reinforced composite materials [2, 19, 25–27], however, have shown only moderate improvement of mechanical properties. This is mainly because the CNTs are often pulled out [2, 21, 22] due to weak van der Waals interactions between the CNTs and the polymeric matrix.

The CNT/polymer interfaces have been strengthened by using a nonionic surfactant as the processing acid to strengthen the CNT/polymer interfacial interaction, which has led to more than a 30% increase in the elastic modulus for 1 wt% CNTs [27]. Molecular dynamics simulations have shown that the shear strength of the CNT/polymer interface increases by a factor between 15 and 30 (depending on the polymer) for 1% carbon atoms on the CNT to form covalent bonds with the polymer matrix [28]. Molecular dynamics simulations have also shown that the CH_3^+ ion bombardment effectively functionalizes the CNT bundle, which has been verified in the experiments with CF_3^+ ion bombardment [29, 30]. The formation of covalent bonds between the CNTs and the polymer matrix during $C_3F_5^+$ ion bombardment also significantly changes the CNT/polymer interface [31].

The functionalization introduces carbon or hydrogen atoms to form covalent bonds with carbon atoms on the CNT. These 'impurity' atoms may affect the mechanical properties of CNTs [32]. Volpe and Cleri modified an orthogonal tight-binding model to study the effect of surface hydrogenization on graphite and CNTs [33]. For graphite, the C–H bond induced local out-of-plane displacement, giving rise to a local tetragonal distortion: the H atom pulled the C atom out of the base plane, as illustrated schematically in figure 1(a). A similar observation has been made for CNTs, as illustrated in figure 1(b). This destroys the perfect atomic structure and may

[5] Authors to whom any correspondence should be addressed.

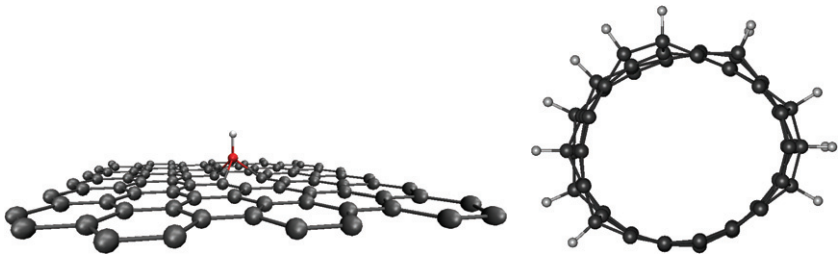

(a) (b)

Figure 1. (a) A schematic diagram to illustrate a hydrogen atom (white) pulling a carbon atom (red) out of the graphene (black); (b) a schematic diagram to illustrate hydrogen atoms (white) forming covalent bonds with carbon atoms (black).

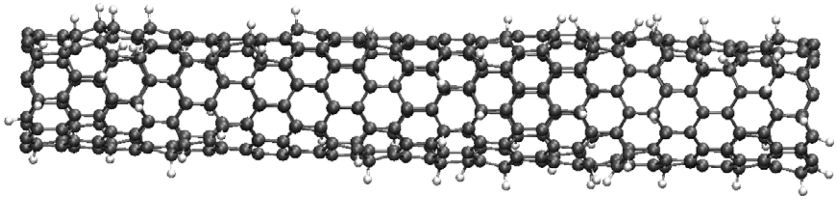

Figure 2. The relaxed structure of the (9, 0) zigzag carbon nanotube with 20% hydrogenization. The white atoms denote hydrogen, and black atoms denote carbon.

significantly reduce the elastic modulus, strength and fracture strain of CNTs.

The CNT elastic modulus decreases gradually with the increasing functionalization [28]. Functionalization may also reduce the critical bulking load by 15% for the CNT in compression [34]. There is, however, no study of functionalization and its effects on the tensile strength and fracture strain of CNTs. The purpose of this paper is to investigate systematically the amount and distribution of CNT functionalization on the elastic modulus, strength and fracture strain of CNTs.

2. Computational model

The atomic-scale finite element method (AFEM) [35, 36] is an order-N atomistic simulation method based on the second-generation interatomic potential for hydrocarbons [37]. It models each atom as a node, and accurately describes the interactions between carbon atoms on the carbon nanotube and between carbon atoms and chemisorbed hydrogen atoms. The total energy in the system is the sum of the energy in all C–C and C–H covalent bonds. The minimization of total energy then gives the atom positions at equilibrium. Similar to the continuum finite element method, AFEM uses both the first- and second-order derivatives of the system energy in energy minimization, and is therefore more effective and robust than the widely used conjugate gradient method.

A hydrogen atom is first placed on the surface of the graphite to form a covalent bond with a carbon atom. The system is then relaxed, which gives the equilibrium C–H bond length $r_{\mathrm{C-H}} = 0.112$ nm. This agrees well with the modified orthogonal tight-binding model (0.111 nm) [33], as well as with the density functional theory calculation (0.112 nm) [38].

The percentage of functionalization is the ratio of the number of hydrogen atoms, N^{H}, to the number of carbon atoms on the CNT, N^{C}, i.e. $N^{\mathrm{H}}/N^{\mathrm{C}}$. Figure 2 shows the simulation results of a (9, 0) zigzag single-wall CNT with 396 carbon atoms and 79 hydrogen atoms, which gives 20% functionalization. Periodic boundary conditions are imposed at the two ends of the CNT, which prescribe the axial strain applied to the CNT.

3. Numerical results

The stress in the CNT is defined by the ratio of total resulting force on all atoms in a cross section to the CNT cross-sectional area $2\pi Rt$, where R is the radius and t is the CNT wall thickness. The interlayer spacing of graphite, 0.34 nm, is taken as the CNT wall thickness in this paper, even though it is unnecessary to define the CNT wall thickness t since the stress always appears together with t via their product, stress $*t$. This is similar to that the Young's modulus E and thickness t of single-wall CNTs always appear together as Et in all experimentally measurable or theoretically calculable properties [39–41], and it is therefore unnecessary to define E and t separately. The prior modeling and simulations of single-wall CNTs can be grouped to two types. One takes the interlayer spacing of graphite (0.34 nm) as the SWNT thickness, and the resulting Young's modulus is around 1 TPa [3, 9–11]. The other is based on the continuum shell modeling, which gives the thickness around 0.066 nm and Young's modulus 5.5 TPa [8, 12–16]. These two types, however, give approximately the same Et, 0.34 TPa nm for the first group and 0.36 TPa nm for the second group.

Figure 3 shows the stress–strain curves for the (9, 0) CNT without functionalization and with 10% functionalization. The two curves are rather close until the functionalized

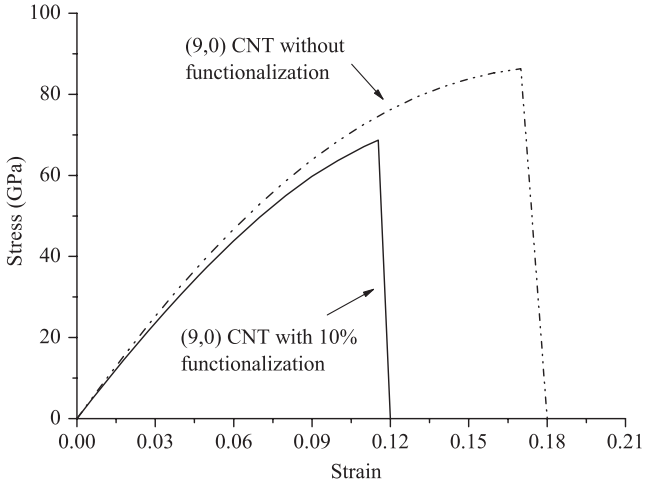

Figure 3. The stress–strain curves of the (9, 0) zigzag CNT with 10% functionalization and without functionalization.

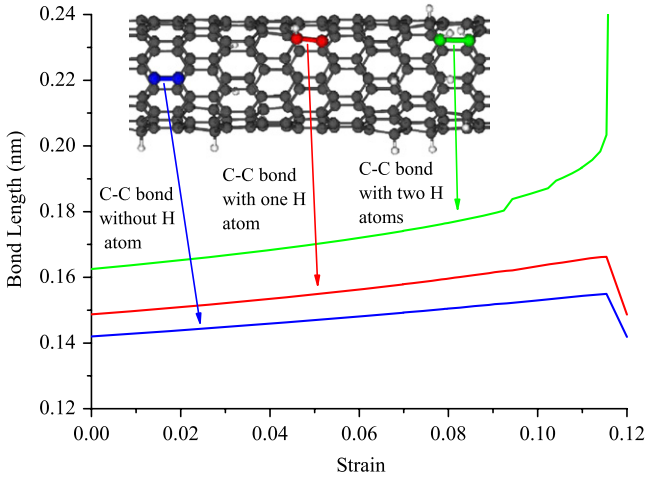

Figure 4. The bond length versus the applied strain for C–C bonds without hydrogen atom, with one H atom and with two H atoms. (This figure is in colour only in the electronic version)

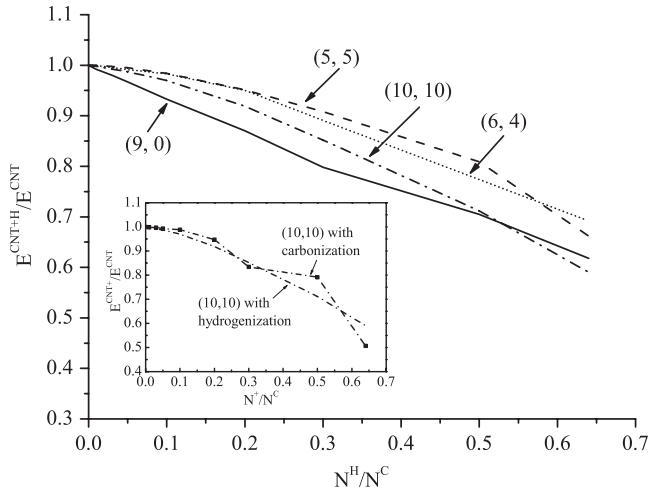

Figure 5. The ratio of elastic moduli of carbon nanotubes, with and without functionalization versus the percentage of functionalization for the (9, 0), (5, 5), (10, 10) and (6, 4) carbon nanotubes. The inset shows the ratio of the elastic modulus of (10, 10) armchair carbon nanotubes, with and without functionalization, versus the percentage of functionalization for hydrogenization and carbonization.

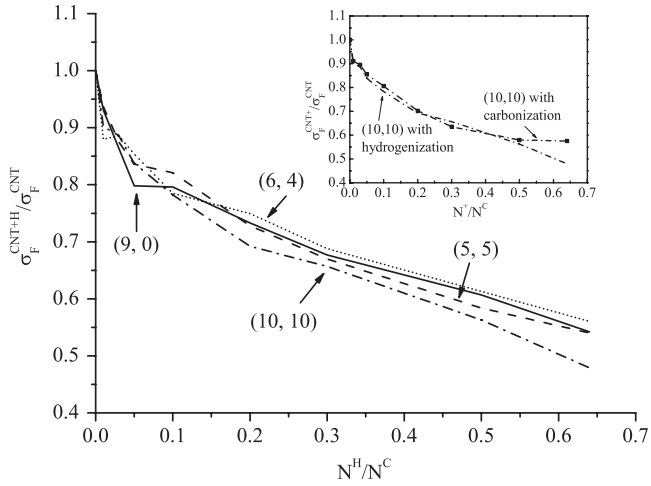

Figure 6. The ratio of strength of carbon nanotubes, with and without functionalization, versus the percentage of functionalization for the (9, 0), (5, 5), (10, 10) and (6, 4) carbon nanotubes. The inset shows the ratio of strength of the (10, 10) armchair carbon nanotubes, with and without functionalization, versus the percentage of functionalization for hydrogenization and carbonization.

CNT reaches its peak stress, which is consistent with the prior studies [28]. Both curves show a rather abrupt drop after the strength (peak stress) is reached. The strength for the functionalized CNT is lower than that without functionalization, and so is the fracture strain. This reduction of peak stress is because the functionalization introduces nonuniformity in the CNT, which leads to localized deformation and early fracture of the CNT, as discussed in the following.

Figure 4 shows the bond length versus the applied strain for C–C bonds (i) without any hydrogen atom, (ii) with one H atom, and (iii) with two H atoms. The hydrogen atoms clearly increase the length of C–C bonds. Once the strain exceeds 11%, the length of the C–C bond with two H atoms increases rapidly, while the lengths of bonds without or with one H atom do not increase (and even decrease). This gives the localized deformation (in the C–C bond with two H atoms), which leads to bond fracture and therefore effectively strength reduction of the CNT.

The elastic modulus E is determined from the initial slope of the stress–strain curve. The strength σ_F and fracture strain ε_F are defined for the point where the peak stress is reached because after this the stress drops sharply,as shown in figure 3, and is similar to brittle fracture. Here the strength and fracture strain are not linearly proportional since the stress–strain curve in figure 3 is nonlinear. The fracture strain is called the ductility of the CNT in the following.

Figures 5–7 show the elastic modulus E, strength σ_F and ductility ε_F of CNTs versus the percentage of functionalization, respectively. Each figure shows four curves for the (9, 0) zigzag, (5, 5) and (10, 10) armchair, and (6, 4) chiral CNTs.

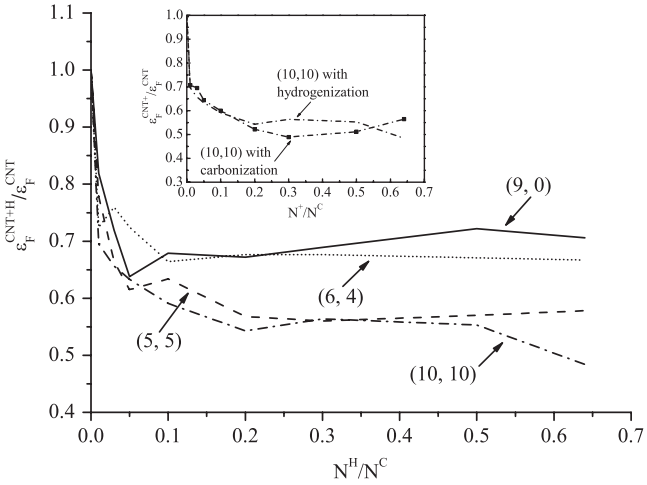

Figure 7. The ratio of ductility of carbon nanotubes, with and without functionalization, versus the percentage of functionalization for the (9, 0), (5, 5), (10, 10) and (6, 4) carbon nanotubes. The inset shows the ratio of ductility of the (10, 10) armchair carbon nanotubes, with and without functionalization, versus the percentage of functionalization for hydrogenization and carbonization.

The (9, 0), (5, 5) and (6, 4) CNTs have approximately the same radius such that their comparison shows the effect of CNT chiralities (helicities). The (5, 5) and (10, 10) CNTs have the same helicity such that their comparison shows the effect of CNT radius.

The elastic modulus E^{CNT+H} of functionalized CNTs is normalized by its counterpart E^{CNT} without functionalization in figure 5. The elastic modulus for each CNT gradually decreases as the functionalization increases, which is consistent with prior studies [28]. As the percentage of functionalization exceeds 10%, the elastic modulus decreases rather quickly as the functionalization increases, reflecting the strong effect of functionalization on the elastic modulus of CNTs. The comparison of curves for (5, 5) and (10, 10) CNTs suggests that the elastic modulus of large CNTs is more sensitive to functionalization than small CNTs. The elastic modulus is also sensitive to the CNT helicity, as seen from the difference between (9, 0), (5, 5) and (6, 4) CNTs.

The strength σ_F^{CNT+H} of functionalized CNTs, normalized by its counterpart σ_F^{CNT} without functionalization, is shown versus the percentage of functionalization in figure 6. The strength drops rather sharply at the small percentage of functionalization, and continues to decrease with the increasing functionalization. This suggests that the strength of CNTs is rather sensitive to functionalization. The curves for (9, 0), (5, 5), (10, 10) and (6, 4) CNTs are rather close in figure 6, which implies that the reduction of CNT strength due to functionalization, $\sigma_F^{CNT+H}/\sigma_F^{CNT}$, is insensitive to the CNT radius and helicity. However, the strength σ_F^{CNT} of CNTs without functionalization depends on the CNT helicity but not radius [42]. Therefore, the strength σ_F^{CNT+H} of a functionalized CNT is sensitive to the helicity and insensitive to the radius.

The ductility ε_F^{CNT+H} of functionalized CNTs, also normalized by its counterpart ε_F^{CNT} without functionalization, is shown versus the percentage of functionalization in figure 7.

Table 1. Effect of clustered C–H bonds.

	Elastic modulus (GPa)	Strength (GPa)	Ductility
No C–H bond	751.66	103.02	0.2683
1 ring	749.50	79.0	0.1363
2 rings	724.90	54.8	0.084
3 rings	709.10	52.7	0.0815

All curves initially drop very sharply, which suggests that the ductility of CNT is sensitive to functionalization. The curves then approach some plateau because the elastic modulus reduction catches up or even exceeds the strength reduction at large functionalization. The curves for (5, 5) and (10, 10) CNTs are essentially the same, but both are lower than the curves for the (9, 0) and (6, 4) CNTs. This implies that the CNT radius has little effect on the ductility reduction $\varepsilon_F^{CNT+H}/\varepsilon_F^{CNT}$ due to functionalization, but the helicity does. Since the ductility ε_F^{CNT} of CNTs without functionalization depends on the CNT helicity but not radius [42], the ductility ε_F^{CNT+H} of functionalized CNTs shows the same behavior.

Figures 5–7 suggest different effects of functionalization on mechanical properties of CNTs. The elastic modulus decreases gradually at small functionalization ($<10\%$) because it represents the average behavior of all atoms. Large functionalization has a strong effect on the elastic modulus. The strength and ductility are sensitive to functionalization because they are controlled by local bond breaking. Small functionalization may cause localized deformation and trigger early bond breaking, therefore significantly reducing the strength and ductility.

Figures 5–7, together with [42], also suggest different effects of chirality on mechanical properties of functionalized CNTs. The strength and ductility of functionalized CNTs are sensitive to the helicity but not radius, while the elastic modulus depends on both.

In order to examine the effect of random distributed C–H bonds on the CNTs, 10 random distributions are realized for each CNT with a given percentage of functionalization. The derivations in ductility reduction and strength reduction are less than 6% and 4%, respectively. Figure 8 shows the extreme case that all functionalizations are clustered together to form one, two or three rings of C–H bonds on the (10, 10) armchair CNT. The elastic modulus, strength and ductility are given in table 1. For comparison, the results for CNTs without functionalization are also shown. The reduction in elastic modulus is relatively small, but the reductions in strength and ductility are quite large, which reflects the effect of clustering. The results for two and three rings are essentially the same, which suggest the two rings of C–H bonds form the weakest link.

The above results are for hydrogenization, i.e. the formation of C–H bonds. We have also investigated carbonization, i.e. the formation of C–C bonds. The insets in figures 5–7 show the elastic modulus, strength and ductility of functionalized (10, 10) armchair CNTs, all normalized by their counterparts without functionalization, versus the percentage of functionalization for both hydrogenization and carbonization. The curves in each figure are essentially the

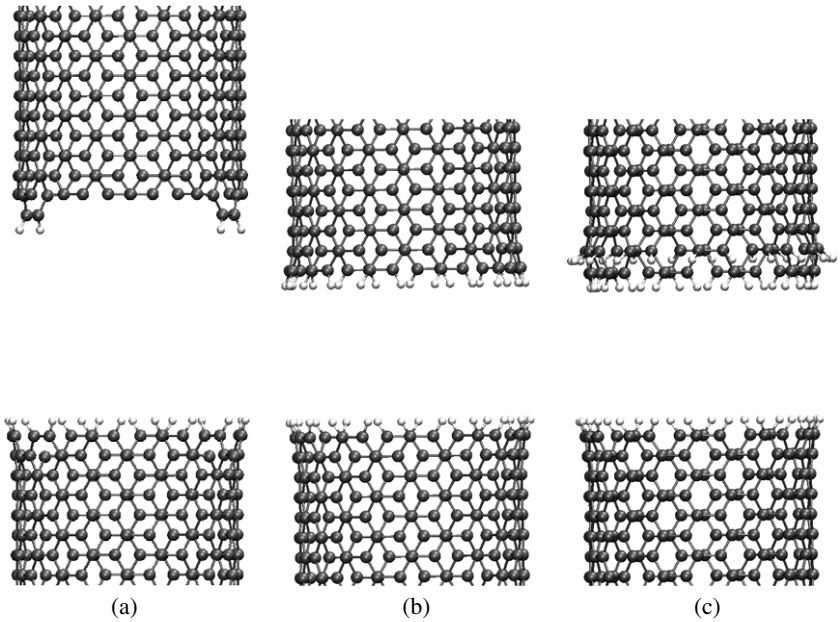

Figure 8. The breaking configurations of carbon nanotubes with (a) one ring, (b) two rings and (c) three rings of C–H bonds. The white atoms denote hydrogen and black atoms denote carbon.

same. Therefore, the hydrogenization and carbonization have the same effect on the mechanical properties of functionalized CNTs.

4. Conclusions

We have used atomistic simulations to study the effect of functionalization (hydrogenization) on the mechanical properties of single-wall carbon nanotubes (CNTs). The functionalization (forming C–H bonds) has little effect on the elastic modulus of CNTs unless the percentage of functionalization exceeds 10%. However, both the strength and ductility drop sharply at a small percentage of functionalization, reflecting their sensitivity to C–H bonds. The cluster of C–H bonds forming two rings leads to significant reduction in the strength and ductility. The effect of functionalization via carbonization is shown to have essentially the same effect as the hydrogenation.

Acknowledgments

BL acknowledges the support from the National Natural Science Foundation of China (grant nos. 10542001, 10702034 and 10732050). KCH acknowledges the support from the National Basic Research Program of China (973 Program) grant no. 2007CB936803. YH acknowledges the support from the NSF through Nano-CEMMS (grant no. DMI03-28162) at the University of Illinois and ONR Composites for Marine Structures Program (grant N00014-01-1-0205, Program Manager Dr Y D S Rajapakse). The support from the NSFC and the Ministry of Education of China is also acknowledged.

References

[1] Gao G H, Cagin T and Goddard W A 1998 Energetics, structure, mechanical and vibrational properties of single-walled carbon nanotubes *Nanotechnology* **9** 184–91
[2] Qian D, Dickey E C, Andrews R and Rantell T 2000 Load transfer and deformation mechanisms in carbon nanotube-polystyrene composites *Appl. Phys. Lett.* **76** 2868–70
[3] Li C Y and Chou T W 2003 A structural mechanics approach for the analysis of carbon nanotubes *Int. J. Solids Struct.* **40** 2487–99
[4] Treacy M M J, Ebbesen T W and Gibson J M 1996 Exceptionally high Young's modulus observed for individual carbon nanotubes *Nature* **381** 678–80
[5] Wong E W, Sheehan P E and Lieber C M 1997 Nanobeam mechanics: elasticity, strength, and toughness of nanorods and nanotubes *Science* **277** 1971–5
[6] Yu M F, Lourie O, Dyer M J, Moloni K, Kelly T F and Ruoff R S 2000 Strength and breaking mechanism of multiwalled carbon nanotubes under tensile load *Science* **287** 637–40
[7] Yu M F, Files B S, Arepalli S and Ruoff R S 2000 Tensile loading of ropes of single wall carbon nanotubes and their mechanical properties *Phys. Rev. Lett.* **84** 5552–5
[8] Yakobson B I, Brabec C J and Bernholc J 1996 Nanomechanics of carbon tubes: instabilities beyond linear response *Phys. Rev. Lett.* **76** 2511–4
[9] Lu J P 1997 Elastic properties of carbon nanotubes and nanoropes *Phys. Rev. Lett.* **79** 1297–300
[10] Hernandez E, Goze C, Bernier P and Rubio A 1998 Elastic properties of C and $B_xC_yN_z$ composite nanotubes *Phys. Rev. Lett.* **80** 4502–5
[11] Jin Y and Yuan F G 2003 Simulation of elastic properties of single-walled carbon nanotubes *Compos. Sci. Technol.* **63** 1507–15
[12] Zhou X, Zhou J J and Ou-Yang Z C 2000 Strain energy and Young's modulus of single-wall carbon nanotubes calculated from electronic energy-band theory *Phys. Rev.* B **62** 13692–6

[13] Kudin K N, Scuseria G E and Yakobson B I 2001 C2F, BN, and C nanoshell elasticity from *ab initio* computations *Phys. Rev.* B **64** 235406
[14] Tu Z C and Ou-Yang Z 2002 Single-walled and multiwalled carbon nanotubes viewed as elastic tubes with the effective Young's moduli dependent on layer number *Phys. Rev.* B **65** 233407
[15] Pantano A, Boyce M C and Parks D M 2003 Nonlinear structural mechanics based modeling of carbon nanotube deformation *Phys. Rev. Lett.* **91** 145504
[16] Wang L F, Zheng Q S, Liu J Z and Jiang Q 2005 Size dependence of the thin-shell model for carbon nanotubes *Phys. Rev. Lett.* **95** 105501
[17] Belytschko T, Xiao S P, Schatz G C and Ruoff R S 2002 Atomistic simulations of nanotube fracture *Phys. Rev.* B **65** 235430
[18] Yakobson B I, Campbell M P, Brabec C J and Bernholc J 1997 High strain rate fracture and C-chain unraveling in carbon nanotubes *Comput. Mater. Sci.* **8** 341–8
[19] Wagner H D, Lourie O, Feldman Y and Tenne R 1998 Stress-induced fragmentation of multiwall carbon nanotubes in a polymer matrix *Appl. Phys. Lett.* **72** 188–90
[20] Jin Z, Pramoda K P, Xu G and Goh S H 2001 Dynamic mechanical behavior of melt-processed multi-walled carbon nanotube/poly(methyl methacrylate) composites *Chem. Phys. Lett.* **337** 43–7
[21] Bower C, Rosen R, Jin L, Han J and Zhou O 1999 Deformation of carbon nanotubes in nanotube-polymer composites *Appl. Phys. Lett.* **74** 3317–9
[22] Ajayan P M, Schadler L S, Giannaris C and Rubio A 2000 Single-walled carbon nanotube-polymer composites: strength and weakness *Adv. Mater.* **12** 750–3
[23] Jin L, Bower C and Zhou O 1998 Alignment of carbon nanotubes in a polymer matrix by mechanical stretching *Appl. Phys. Lett.* **73** 1197–9
[24] Haggenmueller R, Gommans H H, Rinzler A G, Fischer J E and Winey K I 2000 Aligned single-wall carbon nanotubes in composites by melt processing methods *Chem. Phys. Lett.* **330** 219–25
[25] Shaffer M S P and Windle A H 1999 Fabrication and characterization of carbon nanotube/poly(vinyl alcohol) composites *Adv. Mater.* **11** 937–41
[26] Schadler L S, Giannaris S C and Ajayan P M 1998 Load transfer in carbon nanotube epoxy composites *Appl. Phys. Lett.* **73** 3842–4
[27] Gong X Y, Liu J, Baskaran S, Voise R D and Young J S 2000 Surfactant-assisted processing of carbon nanotube/polymer composites *Chem. Mater.* **12** 1049–52
[28] Frankland S J V, Caglar A, Brenner D W and Griebel M 2002 Molecular simulation of the influence of chemical cross-links on the shear strength of carbon nanotube–polymer interfaces *J. Phys. Chem.* B **106** 3046–8
[29] Ni B and Sinnott S B 2000 Chemical functionalization of carbon nanotubes through energetic radical collisions *Phys. Rev.* B **61** R16343–6
[30] Ni B and Sinnott S B 2001 Tribological properties of carbon nanotube bundles predicted from atomistic simulations *Surf. Sci.* **487** 87–96
[31] Hu Y, Jang I and Sinnott S B 2003 Modification of carbon nanotube-polystyrene matrix composites through polyatomic-ion beam deposition: predictions from molecular dynamics simulations *Compos. Sci. Technol.* **63** 1663–9
[32] Stojkovic D, Zhang P and Crespi V H 2001 Smallest nanotube: breaking the symmetry of sp^3 bonds in tubular geometries *Phys. Rev. Lett.* **87** 125502
[33] Volpe M and Cleri F 2003 Chemisorption of atomic hydrogen in graphite and carbon nanotubes *Surf. Sci.* **544** 24–34
[34] Garg A and Sinnott S B 1998 Effect of chemical functionalization on the mechanical properties of carbon nanotubes *Chem. Phys. Lett.* **295** 273–8
[35] Liu B, Huang Y, Jiang H, Qu S and Hwang K C 2004 The atomic-scale finite element method *Comput. Methods Appl. Mech. Eng.* **193** 1849–64
[36] Liu B, Jiang H, Huang Y, Qu S, Yu M F and Hwang K C 2005 Atomic-scale finite element method in multiscale computation with applications to carbon nanotubes *Phys. Rev.* B **72** 035435
[37] Brenner D W, Shenderova O A, Harrison J A, Stuart S J, Ni B and Sinnott S B 2002 A second-generation reactive empirical bond order (REBO) potential energy expression for hydrocarbons *J. Phys.: Condens. Matter* **14** 783–802
[38] Letardi S, Celino M, Cleri F and Rosato V 2002 Atomic hydrogen adsorption on a Stone–Wales defect in graphite *Surf. Sci.* **496** 33–8
[39] Huang Y, Wu J and Hwang K C 2006 Thickness of graphene and single-wall carbon nanotubes *Phys. Rev.* B **74** 245413
[40] Wu J, Hwang K C and Huang Y 2008 An atomistic-based finite-deformation shell theory for single-wall carbon nanotubes *J. Mech. Phys. Solids* **56** 279–92
[41] Khang D Y, Xiao J L, Kocabas C, MacLaren S, Banks T, Jiang H Q, Huang Y Y G and Rogers J A 2008 Molecular scale buckling mechanics on individual aligned single-wall carbon nanotubes on elastomeric substrates *Nano Lett.* **8** 124–30
[42] Dumitrica T, Hua M and Yakobson B I 2006 Symmetry-, time-, and temperature-dependent strength of carbon nanotubes *Proc. Natl Acad. Sci. USA* **103** 6105–9